



# Molecular Polar Surface Area, Total Solvent Accessible Surface Area (SASA), Heat of Formation, and Gamma-Ray Attenuation Properties of Some Flavonoids

Huseyin Ozan Tekin<sup>1,2\*</sup>, Ghada ALMisned<sup>3</sup>, Shams A. M. Issa<sup>4,5</sup>, Emel Serdaroglu Kasikci<sup>6,7</sup>, Mahreen Arooj<sup>8</sup>, Antoaneta Ene<sup>9\*</sup>, M. S. Al-Buriah<sup>10</sup>, Muhsin Konuk<sup>11</sup> and Hesham M. H. Zakaly<sup>5,12\*</sup>

## OPEN ACCESS

### Edited by:

Carmelo Corsaro,  
University of Messina, Italy

### Reviewed by:

D. K. Gaikwad,  
Shri Shivaji Vidy Prasarak Sanstha's  
Arts, Commerce and Science College,  
India  
Iskender Akkurt,  
Süleyman Demirel University, Turkey

### \*Correspondence:

Hesham M. H. Zakaly  
h.m.zakaly@gmail.com  
Antoaneta Ene  
antoaneta.ene@ugal.ro  
Huseyin Ozan Tekin  
tekin765@gmail.com

### Specialty section:

This article was submitted to  
Atomic and Molecular Physics,  
a section of the journal  
Frontiers in Physics

**Received:** 18 December 2021

**Accepted:** 27 January 2022

**Published:** 07 March 2022

### Citation:

Tekin HO, ALMisned G, Issa SAM,  
Kasikci ES, Arooj M, Ene A,  
Al-Buriah MS, Konuk M and  
Zakaly HMH (2022) Molecular Polar  
Surface Area, Total Solvent Accessible  
Surface Area (SASA), Heat of  
Formation, and Gamma-Ray  
Attenuation Properties of  
Some Flavonoids.  
Front. Phys. 10:838725.  
doi: 10.3389/fphy.2022.838725

<sup>1</sup>Medical Diagnostic Imaging Department, College of Health Sciences, University of Sharjah, Sharjah, United Arab Emirates, <sup>2</sup>Istinye University, Faculty of Engineering and Natural Sciences, Computer Engineering Department, Istanbul, Turkey, <sup>3</sup>Department of Physics, College of Science, Princess Nourah Bint Abdulrahman University, Riyadh, Saudi Arabia, <sup>4</sup>Physics Department, Faculty of Science, University of Tabuk, Tabuk, Saudi Arabia, <sup>5</sup>Physics Department, Faculty of Science, Al-Azhar University, Assiut, Egypt, <sup>6</sup>Department of Molecular Biology and Genetics, Faculty of Engineering and Natural Sciences, Uskudar University, Istanbul, Turkey, <sup>7</sup>Department of Molecular Biology and Genetics, Faculty of Engineering and Natural Sciences, Neuropsychopharmacology Research and Application Center, Uskudar University, Istanbul, Turkey, <sup>8</sup>Chemistry Department, College of Sciences, University of Sharjah, Sharjah, United Arab Emirates, <sup>9</sup>INPOLDE Research Center, Department of Chemistry, Physics and Environment, Faculty of Sciences and Environment, Dunarea de Jos University of Galati, Galati, Romania, <sup>10</sup>Department of Physics, Sakarya University, Sakarya, Turkey, <sup>11</sup>Department of Molecular Biology and Genetics, Faculty of Engineering and Natural Sciences, Uskudar University, Istanbul, Turkey, <sup>12</sup>Institute of Physics and Technology, Ural Federal University, Ekaterinburg, Russia

The chemical and physical characteristics of several flavonoid compounds such as geraniol, thymoquinone, betaine, apigenin, N-acetylcysteine, catechin, L-carnosine, epigallocatechin, and saponarin were examined in this work. Numerous molecular properties of all flavonoid compounds used in this study were calculated using the Calculate Molecular Properties module of Accelrys Discovery Studio v20.1.0.19295.0. These properties included molecular polar surface area, total solvent accessible surface area, and heat of formation. We used the MCNPX general-purpose Monte Carlo code in combination with the Phy-X PSD software to determine gamma-ray interaction parameters such as attenuation coefficients, effective atomic numbers, and buildup factors. The findings indicate that the flavonoids' elemental compositions have a direct effect on their chemical and physical properties. Additionally, a synergistic interaction of chemical and physical behaviors has been observed. Among the flavonoids studied, saporanin was shown to have the highest polar surface area and solvent accessible surface area, as well as the highest stability. Additionally, saporanin had the strongest gamma-ray attenuation characteristics across a broad photon energy range. It may be inferred that saporanin's elemental structure enables a synergistic relationship between its chemical and physical characteristics. The findings of this study may contribute to the evaluation of saporanin's hypoglycemic, antibacterial, and hepatoprotective effects.

**Keywords:** flavonoids, chemical properties, radiation attenuation, polar surface area, SASA

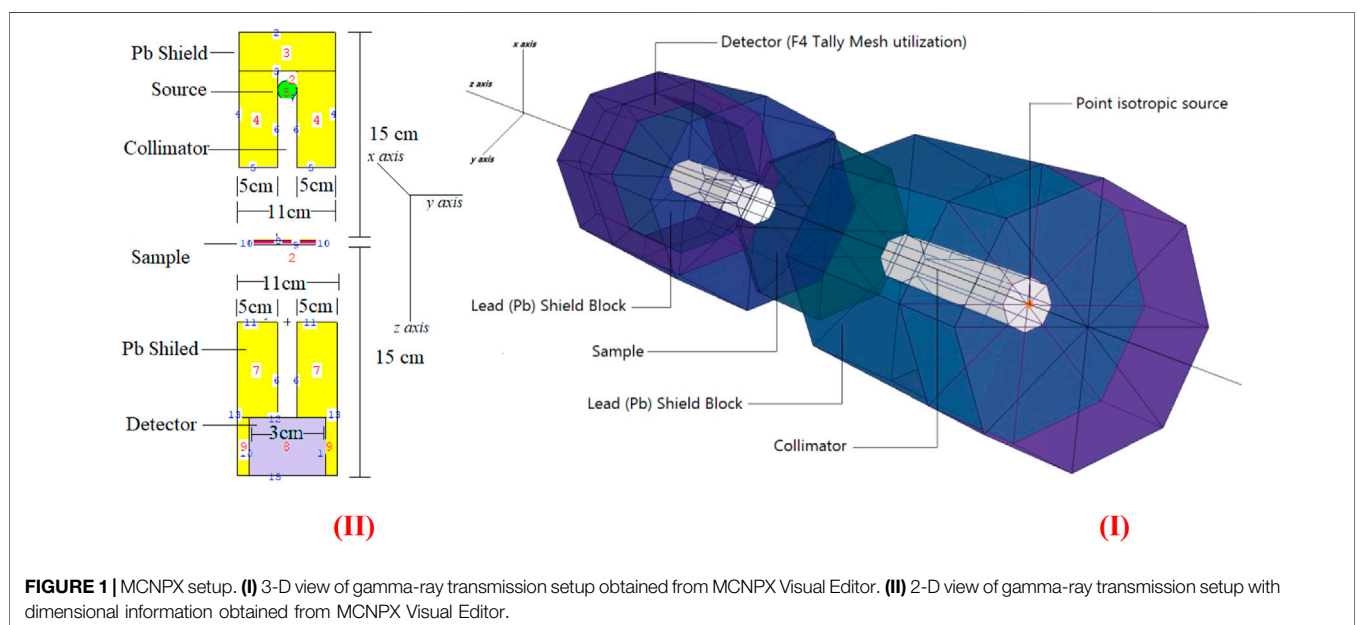
## INTRODUCTION

Free radicals contain one or more un-shared electrons in their outer orbits [1, 2]. They exist as both organic and inorganic molecules. Free radicals react with unsaturated fatty acids, DNA molecules, and sulfhydryl bonds in protein molecules and damage cells and tissues [2, 3]. The active property of radicals is related to the diffusion distance. Since hydroxyl radical is extremely active, it reacts immediately where it is formed without the need for diffusion farther from the cell part where it occurs. Hydrogen peroxide ( $H_2O_2$ ), on the other hand, diffuses easily from mitochondrial membranes, peroxisomal membranes, and plasma membranes and can show its toxic effect in cell sections farther from the point where it is released [3]. Every cell that makes up our body has a defense mechanism against radicals, which we call a radical scavenging enzyme system consisting of enzymes such as superoxide dismutase (SOD), catalase (CAT), glutathione peroxidase (GSH-Px), and glutathione reductase (GSSGR). In addition, there is an auxiliary defense mechanism consisting of antioxidant vitamins A, E, C, and lipoic acid [4–6].

Flavonoids are polyphenolic compounds and are structures of plant origin. Four thousand different flavonoids have been described so far. Flavonoids are grouped as flavonols, flavones, flavanones, anthocyanidins, and isoflavonoids [5, 6]. Flavonoids have various biological effects in the cell system and have been reported to have anti-antineoplastic, anti-mutagenic, anti-inflammatory, antioxidant, and antiplatelet activities [5]. Flavonoids can inhibit reactive oxygen species (ROS) damage. They can be used as a direct defender against free radicals [7–10]. Many *in vitro* and *in vivo* studies have reported that flavonoids and phenolic compounds exert antioxidant effects [5, 10]. Normal and man-made ionizing radiation occurs in our world. Exposure to elevated doses of radiation, such as in radiation treatment for cancer, can lead to brain injury and cognitive decline. Study results indicate that chronic exposure to low doses of ionizing [e.g., repetitive x-rays and computed tomography (CT) scans] and non-ionizing radiation (e.g., mobile devices) can trigger severe brain neuropathological changes. As a consequence, living biological tissues may be affected by exposure to radiation [11–15]. Flavonoids are beneficial as antioxidants, are

**TABLE 1** | Chemical compositions and density for studied materials samples.

Code	Materials	Molecular formula	H	C	N	O	S	Density (g/cm <sup>3</sup> )
S1	Geraniol	C <sub>10</sub> H <sub>18</sub> O	0.117618	0.778659	—	0.103722	—	0.867
S2	Betaine	C <sub>5</sub> H <sub>11</sub> NO <sub>2</sub>	0.094644	0.512643	0.119565	0.273149	—	1.000
S3	Thymoquinone	C <sub>10</sub> H <sub>12</sub> O <sub>2</sub>	0.073660	0.731468	—	0.194872	—	1.065
S4	L-Carnosine	C <sub>9</sub> H <sub>14</sub> N <sub>4</sub> O <sub>3</sub>	0.062374	0.477817	0.247649	0.212161	—	1.376
S5	N-Acetylcysteine	C <sub>5</sub> H <sub>9</sub> NO <sub>3</sub> S	0.049717	0.370277	0.086360	0.295939	0.197707	1.480
S6	Apigenin	C <sub>15</sub> H <sub>10</sub> O <sub>5</sub>	0.037298	0.666682	—	0.296021	—	1.548
S7	Catechin	C <sub>15</sub> H <sub>14</sub> O <sub>6</sub>	0.048613	0.620675	—	0.330711	—	1.593
S8	Epigallocatechin	C <sub>15</sub> H <sub>14</sub> O <sub>7</sub>	0.046074	0.588252	—	0.365674	—	1.695
S9	Saponarin	C <sub>27</sub> H <sub>30</sub> O <sub>15</sub>	0.050861	0.545471	—	0.403668	—	1.800



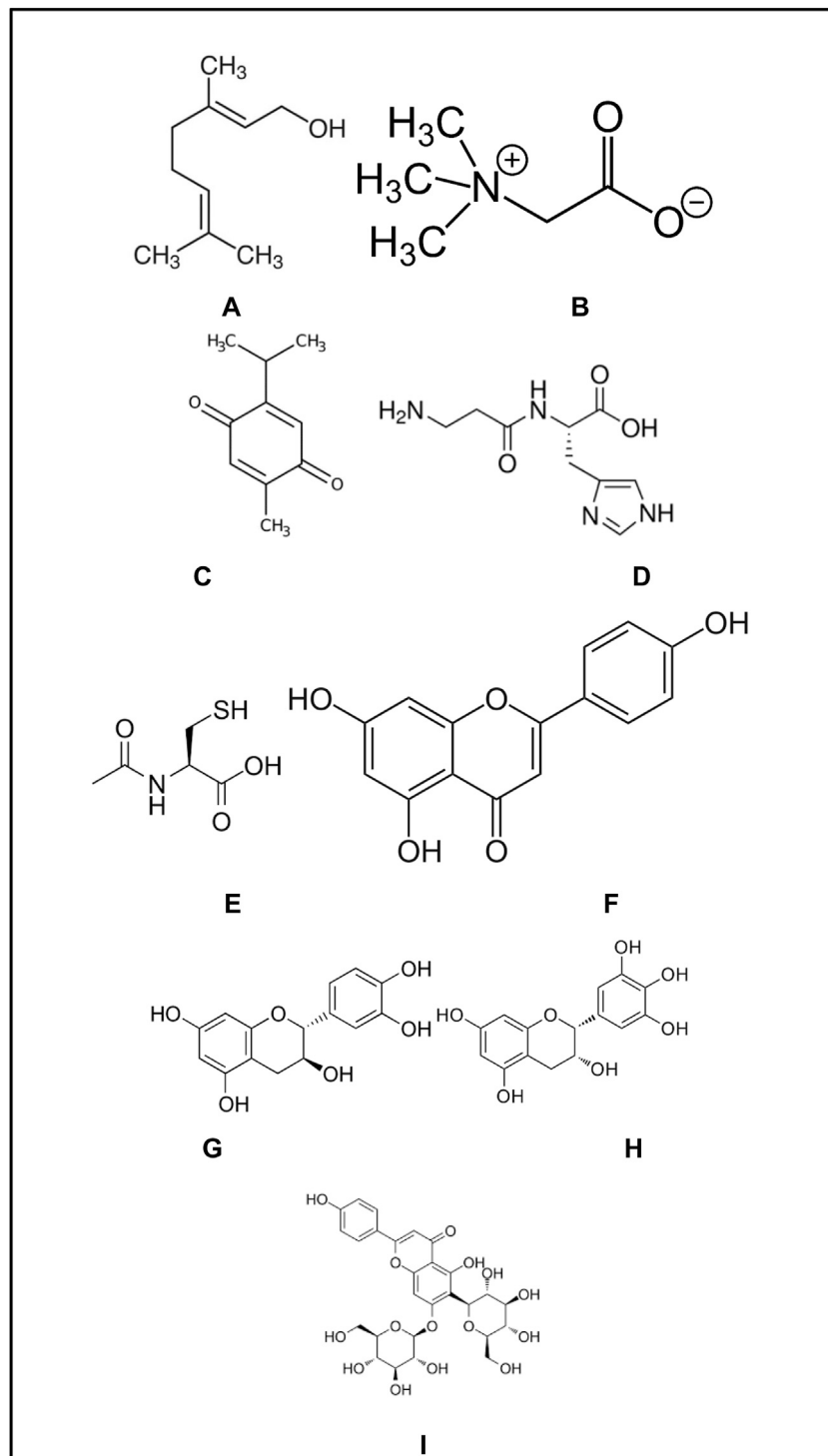


**FIGURE 2** | Molecular structures of investigated flavonoids. **(A)** Geraniol. **(B)** Betaine. **(C)** Thymoquinone. **(D)** L-Carnosine. **(E)** N-Acetylcysteine. **(F)** Apigenin. **(G)** Catechin. **(H)** Epigallocatechin. **(I)** Saponarin.

anti-inflammatory, and are radioprotective. Flavonoids and metabolites will diffuse through the capillary endothelium, the basement membrane, and the glial membrane, which will pass the blood–brain barrier. Preliminary analyses have shown that

epigallocatechin (EGC) and the metabolites such as Flavin can cross the blood–brain barrier and lead to neurogenesis [16–20].

The review of the literature revealed that several researchers have conducted promising studies on the radioprotective

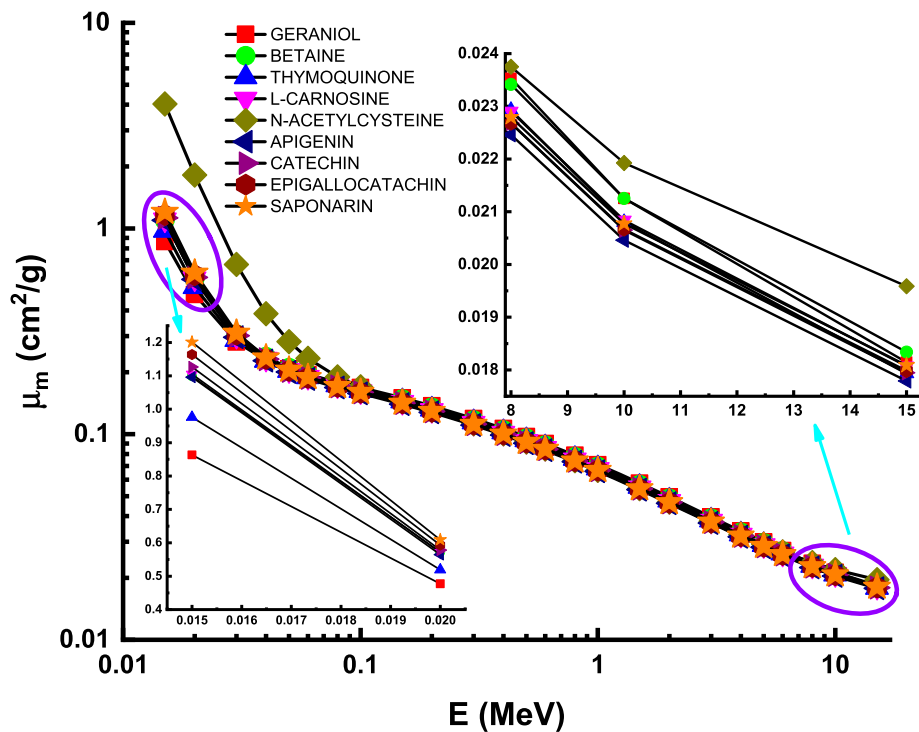


**FIGURE 3** | Variation of mass attenuation coefficient ( $\mu_m$ ) against photon energy for all studied materials.

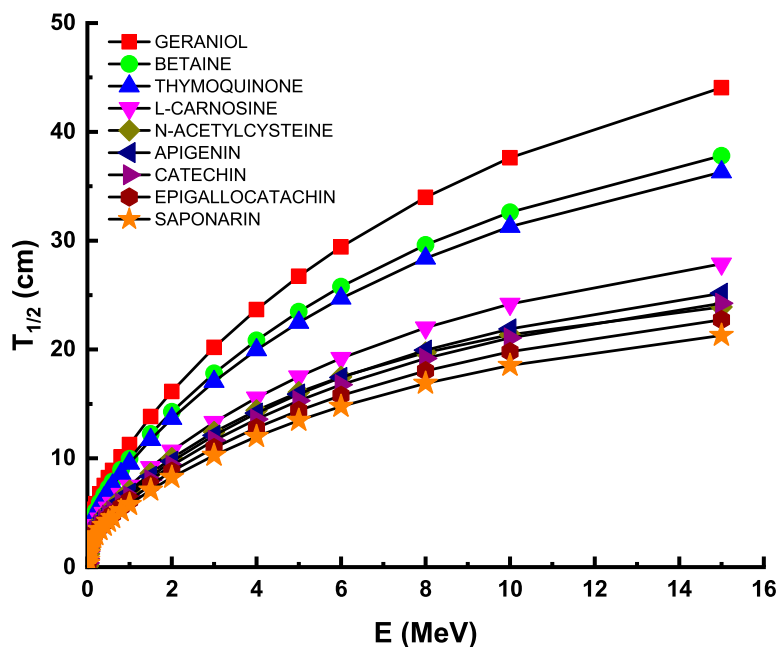


**FIGURE 4** | Variation of half value layer ( $T_{1/2}$ ) against photon energy for all studied materials.

properties of flavonoids [21]. However, no research has been published on the chemical and gamma-ray attenuation characteristics of the flavonoid samples such as geraniol, betaine, thymoquinone L-carnosine, N-acetylcysteine, apigenin,

catechin, epigallocatechin, and saponarin [22–35]. As a result, we used advanced Monte Carlo simulation techniques and mathematical methods to evaluate the crucial molecular characteristics and gamma-ray attenuation capabilities of the

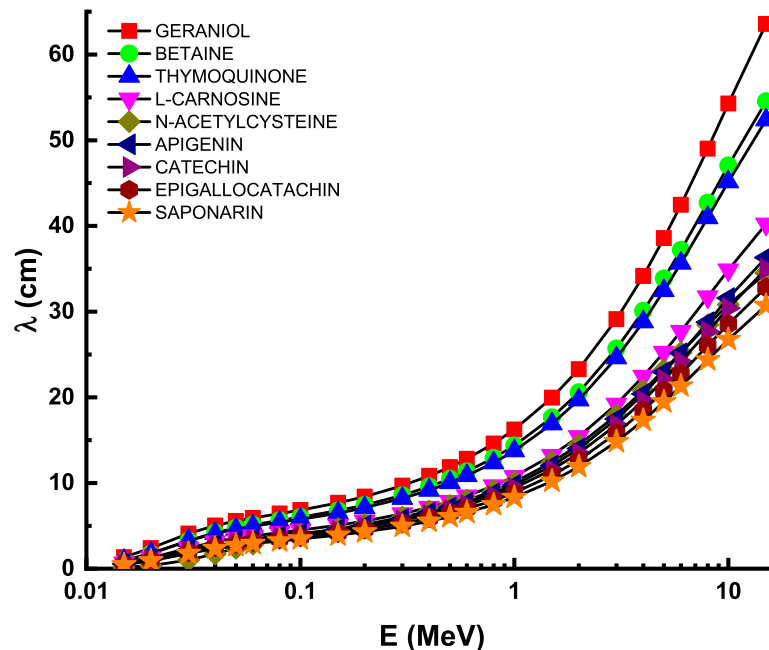


**FIGURE 5** | Variation of mean free path ( $\lambda$ ) against photon energy for all studied materials.

abovementioned flavonoids. Additionally, we expected a synergistic impact of structural modifications on the chemical and physical properties of the flavonoids investigated. The results from this study may assist future research in areas such as the attenuation characteristics of next-generation biomaterials, pharmacology, food science, and food production. Additionally, the results would be applicable to investigations involving radiotherapy and radiology, as well as antioxidant consumption undertaken before and after radiation treatment applications.

## MATERIALS AND METHODS

### Monte Carlo Simulations

This study utilized the MCNPX [36] general-purpose Monte Carlo code for gamma-ray transmission simulations of geraniol, thymoquinone, betaine, apigenin, N-acetylcysteine, catechin, L-carnosine, epigallocatechin, and saponarin samples. Accordingly, mass attenuation coefficients (MAC) of the aforementioned samples were determined at 0.015–10 MeV photon energy range. At first, INPUT files, cell cards, and surface cards were prepared using elemental mass fractions (%wt.) and material densities (see Table 1). The ideal states of these materials were specified during the definition of the investigated flavonoid samples. The term “ideal” refers to a reduction material that is totally composed of the molecular structure of the relevant sample and has no material deficiencies. Of course, providing this condition for experimental investigations is quite challenging. To begin, we defined the simulation equipment’s CELL structures by specifying their covering surfaces and densities. Additionally, the CELL card component has been developed for each

glass sample based on their elemental compositions, which are specified in detail in the material IDs (Mn) section, taking their elemental mass fractions into consideration. Following that, the geometrical alignments of the glass attenuator material’s surfaces were input, as well as the geometrical structures of the surfaces, which may be flat, spherical, or cone shaped. We included radioisotope energies (from 0.015 MeV to 15 MeV, respectively) to the DATA card area, as well as the source geometry as point isotropic. The total geometry of the well-developed simulation system is shown in Figure 1. Furthermore, we added a vital specification to the DATA card, which is expressed as TALLY MESH, for the data collection method. The modeled gamma-ray transmission setup’s outcome function was created in this study using the MCNPX’s F4 TALLY MESH. The F4 tally is used to determine the average flow through a location. The flavonoid samples were determined considering their material properties. In addition, a widely established variance reduction strategy, called tracking-optimization, was also employed. To preserve simulation performance, neutron and electron tracking is disabled and photon tracking is enabled in parameter specification (i.e., imp: p). It is worth mentioning that all the simulation studies were performed using Lenovo® ThinkStation-P620/30E0008QUS Workstation-1X AMD-Ryzen, Threadripper PRO Hexadeca-core (16 Core) 3955 W × 3.90 GHz - 32 GB DDR4 SDRAM RAM.

### Calculation of Molecular Properties

Theoretical calculations were carried out for the compounds using density functional theory (DFT), which provides reasonably high accuracy at an adequate computational cost. First, optimization of compounds in the gas phase was performed using B3LYP/6–31+G (d). The B3LYP hybrid density functional is a common general-purpose method used for ground-state

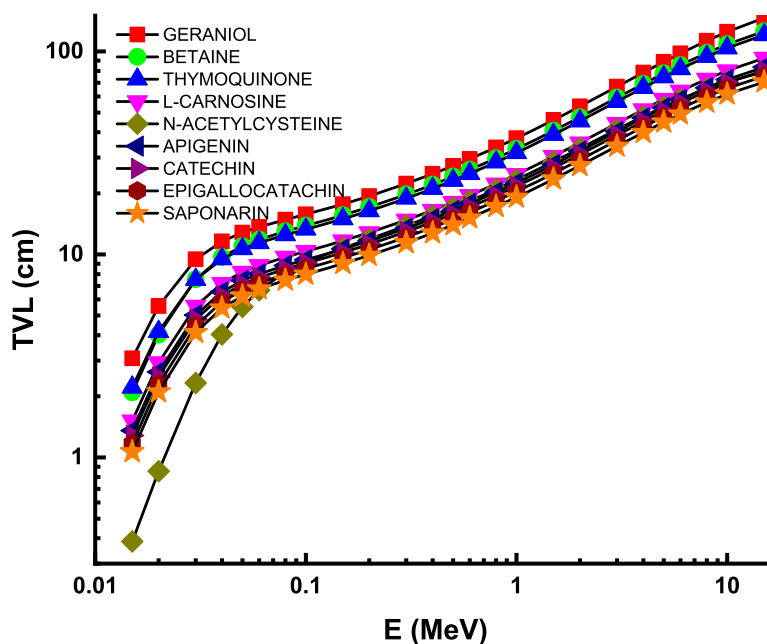


**FIGURE 6** | Variation of 10th value layer (TVL) against photon energy for all studied materials.

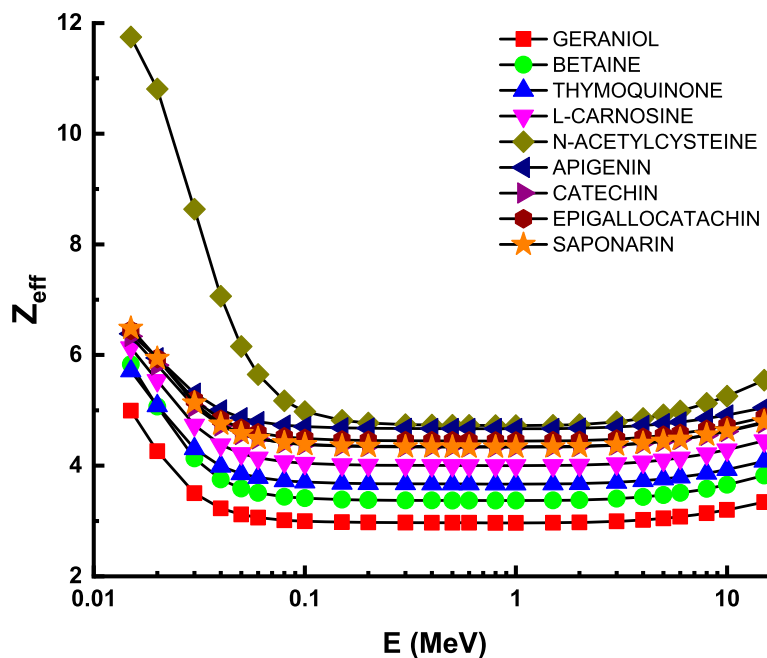


**FIGURE 7** | Variation of effective atomic number ( $Z_{\text{eff}}$ ) against photon energy for all studied materials.

geometry optimization. After the optimization process, compounds were then subjected to compute a number of molecular properties. Various molecular properties, including molecular polar surface area, total solvent accessible surface area

(SASA), and heat of formation of all flavonoid compounds used in this study, were calculated using the Calculate Molecular Properties module of Accelrys Discovery Studio (DS) v20.1.0.19295.0. Next, VAMP tool was employed to calculate

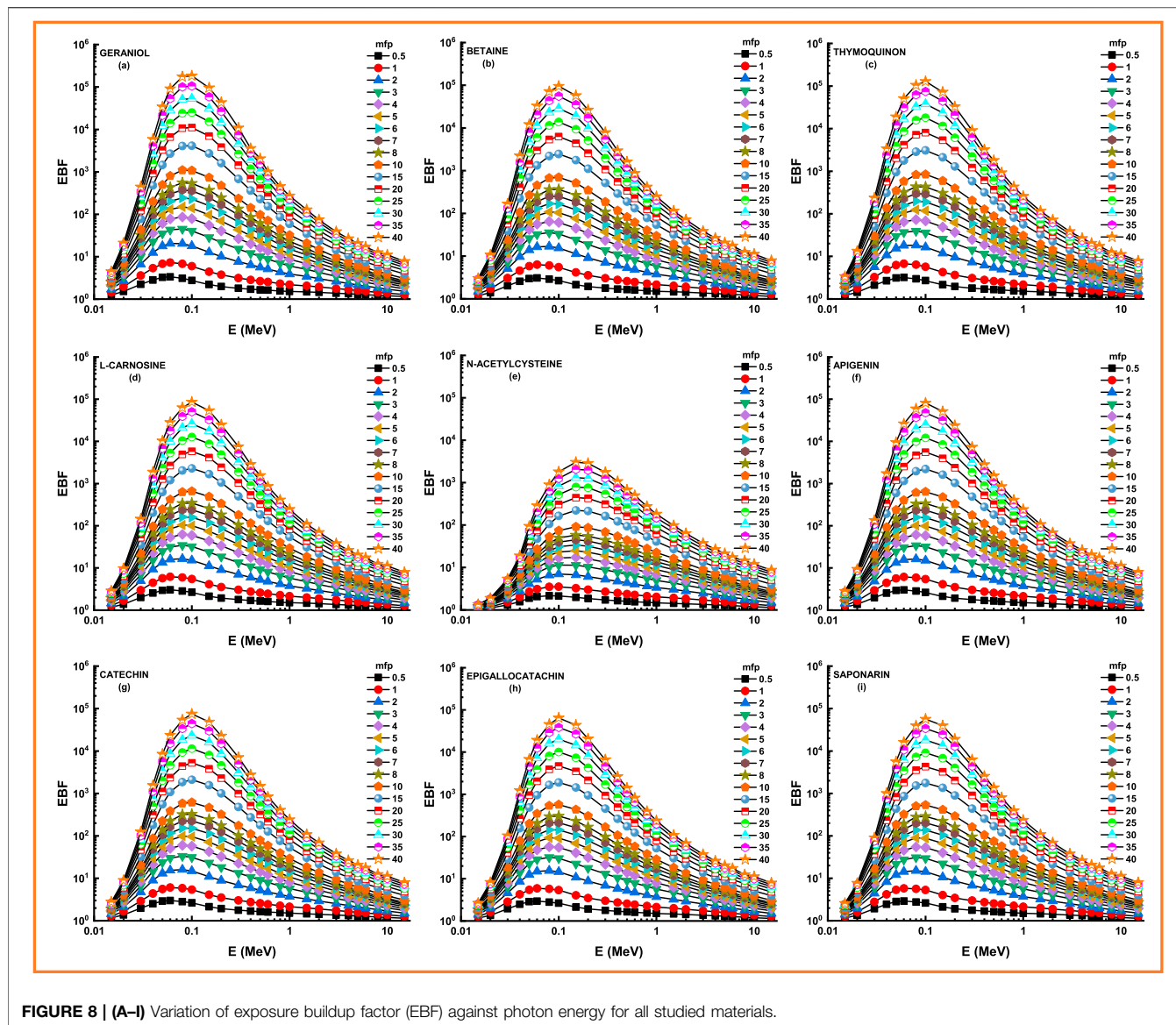


FIGURE 8 | (A–I) Variation of exposure buildup factor (EBF) against photon energy for all studied materials.

the heat of formation for all compounds at the AM1/RHF level [37]. The VAMP tool utilized the single optimized, lowest energy conformation of each compound to compute molecular properties. VAMP is a semi-empirical molecular orbital method, which uses Slater-type atomic orbitals by evaluating the two-electron integrals through a multipole approximation. This method determines a molecular wave function according to the LCAO (Linear Combination of Atomic Orbital) that can then be used to derive various molecular properties.

Flavonoids are neither massive material structures nor physically thick materials in determining their gamma-ray attenuation properties experimentally. This is because experimental gamma-ray studies require the least material thickness to attenuate the incident gamma-rays. In our study, we modeled those flavonoids considering their elemental mass fractions as well as material densities. In this case, it is physically impossible to use them as a solid attenuator material. Therefore,

we performed our simulation studies on a micro-scale by establishing a pure utopic attenuator composed of each flavonoid, respectively. Molecule structures of the investigated flavonoids are also presented in Figure 2.

## RESULTS AND DISCUSSION

### Radiation Attenuation Properties

Researchers are particularly interested in the gamma-ray attenuation characteristics of chemicals and pharmaceuticals to better understand their interactions with ionizing radiation [38–42]. In this study, gamma-ray attenuation properties of studied flavonoids were also calculated in addition to chemical properties. First, mass attenuation coefficients of investigated flavonoid samples were determined *via* MCNPX general-purpose Monte Carlo code. Figure 1 depicts the two-dimensional and

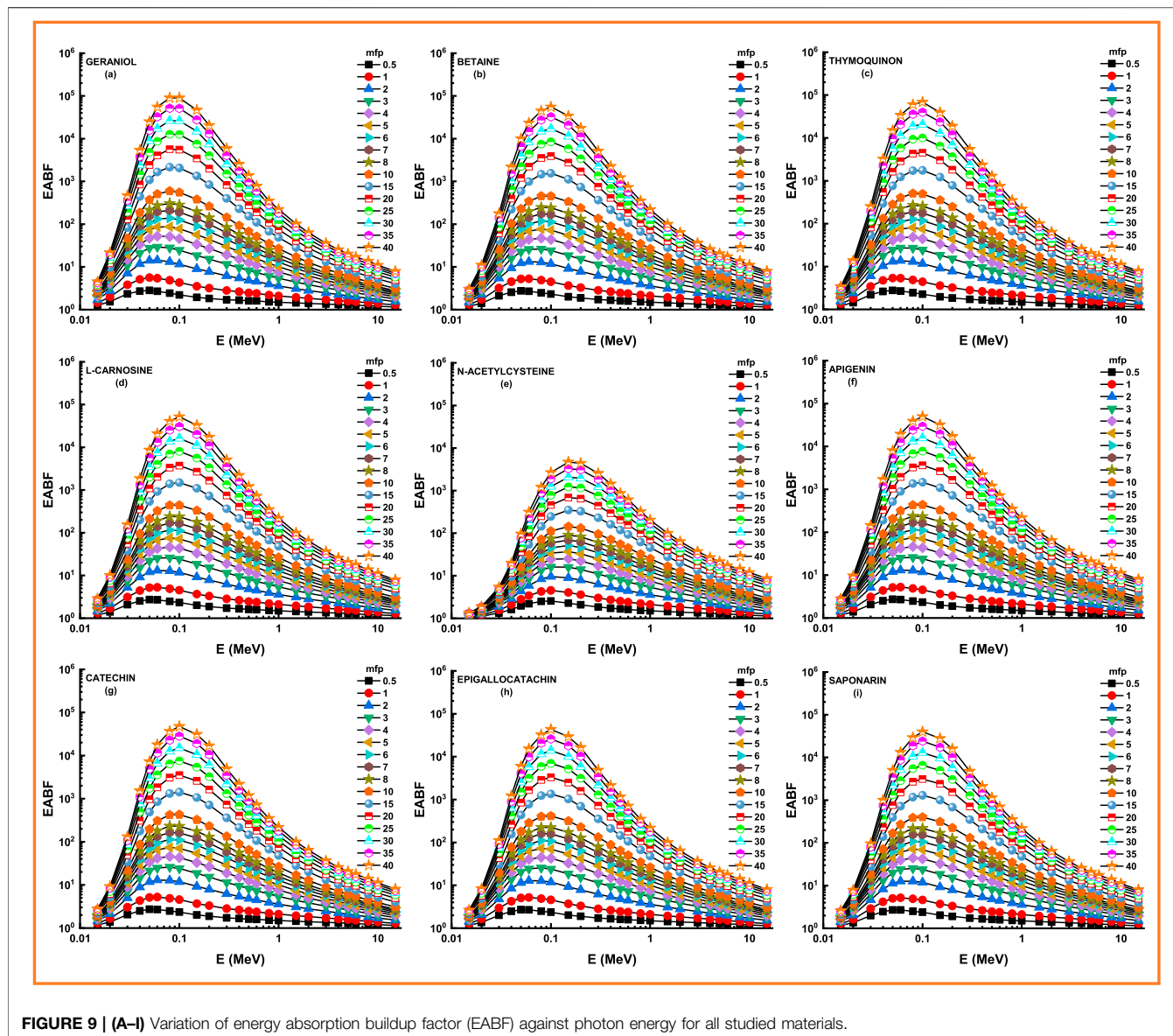
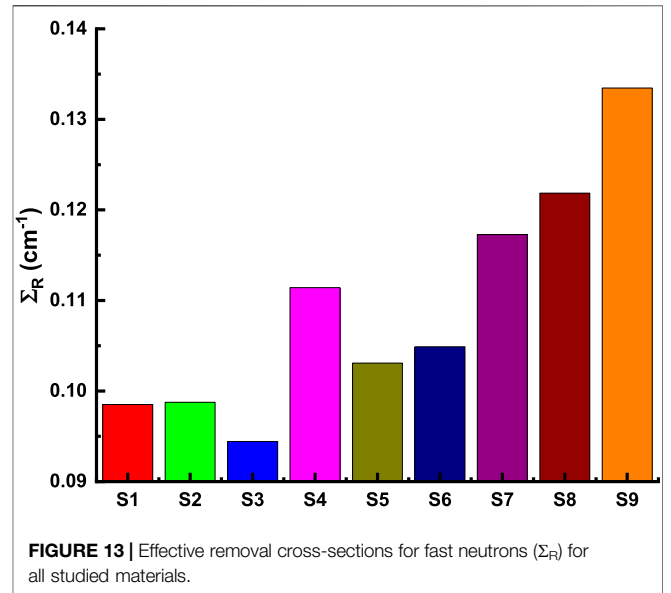
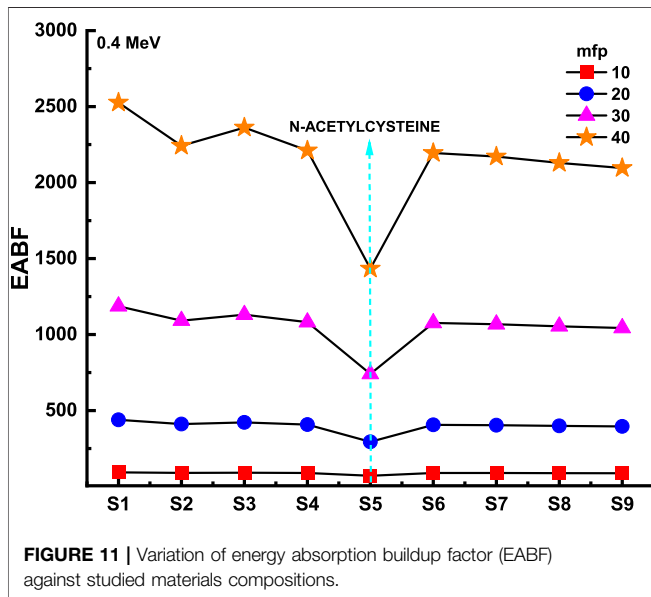
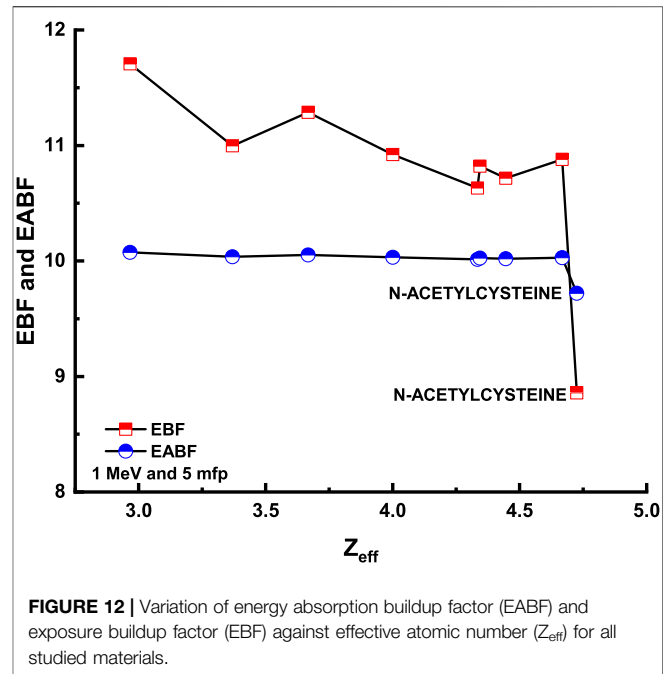
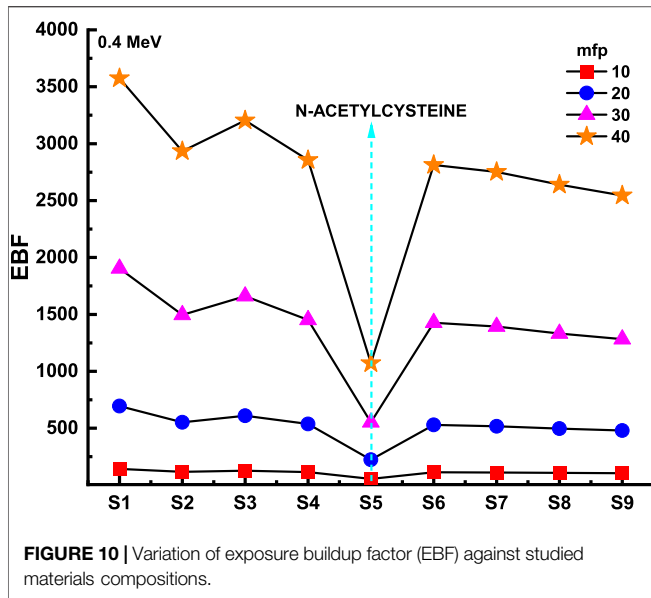


**FIGURE 9 | (A–I)** Variation of energy absorption buildup factor (EABF) against photon energy for all studied materials.

three-dimensional simulation configurations employed, as well as the distances and lengths used for gamma-ray transmission investigations, as acquired using the MCNPX Visual Editor (visedX22S). As seen, a point isotropic gamma-ray source has been embedded in a lead (Pb) block. Primary gamma-rays have been targeted onto an attenuator sample using a collimator. A collimator comparable to that used on the front side of the attenuator was also constructed to avoid backscattered radiation. Finally, near the collimator's end, a detection field employing F4 Tally Mesh (average photon flux at a point or cell) was created to record the intensity of secondary gamma-rays. All equipment was positioned on the  $z$  axis in the simulation setup. The variation of mass attenuation coefficients as a function of incident photon energy is represented in **Figure 3**. Clearly, all the investigated flavonoid samples have a similar attenuation behavior in different energy regions. The highest attenuation can be seen for N-acetylcysteine due to the existence of S element in the chemical composition of this sample

(see **Table 1**). This interesting observation supports the fundamental concepts of gamma interactions with matter [43, 44].

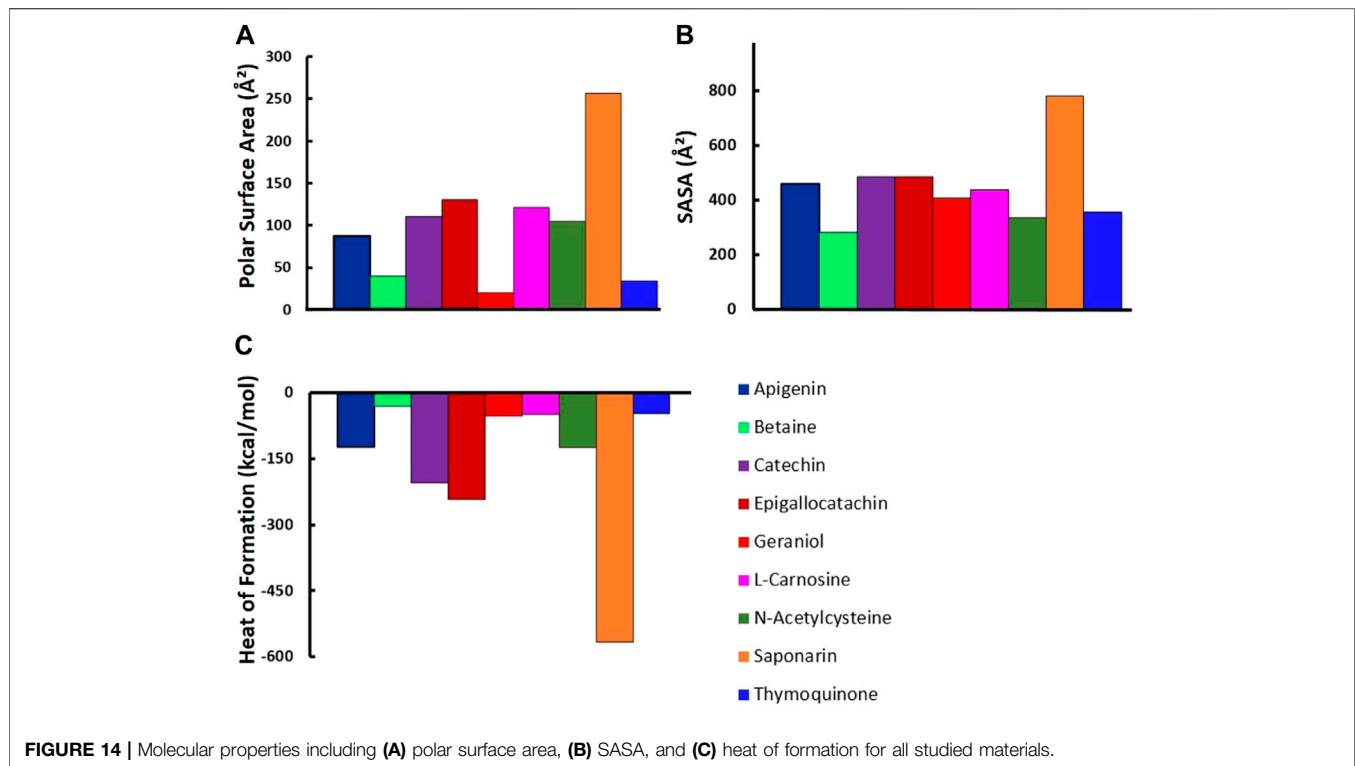
**Figure 4** describes the attenuation properties of the investigated flavonoid samples in terms of half value layer ( $T_{1/2}$ ) as a function of energy up to 15 MeV. The lowest  $T_{1/2}$  and then the highest attenuation occurred at the low energy level (15 keV) with values of 0.926, 0.631, 0.667, 0.456, 0.116, 0.409, 0.386, 0.351, and 0.321 cm for geraniol, betaine, thymoquinone, L-carnosine, N-acetylcysteine, apigenin, catechin, epigallocatechin, and saponarin, respectively. Such observation can be explained according to the photoelectric effect that dominates all the attenuation processes at the low energy levels. **Figure 5** describes the attenuation properties of the investigated flavonoid samples in terms of mean free path ( $\lambda$ ) as a function of energy up to 15 MeV. The highest  $\lambda$  and then the lowest attenuation occurred at the high energy level (15 MeV) with



values of 63.563, 54.535, 52.372, 40.216, 34.496, 36.307, 34.980, 32.807, and 30.716 cm for geraniol, betaine, thymoquinone, L-carnosine, N-acetylcysteine, apigenin, catechin, epigallocatechin, and saponarin, respectively. Such observation can be explained according to the pair production (electron and positron production) that dominates all the attenuation processes at the high energy levels [45, 46].

**Figure 6** describes the attenuation properties of the investigated flavonoid samples in terms of 10th value layer (TVL) as a function of energy up to 15 MeV. The behavior of TVL curve is similar to that of  $T_{1/2}$  and  $\lambda$  at the whole considered energy level [47, 48]. This supports the general variations of the transmission factors with the photon energy, such that all the

transmission factors (TVL,  $T_{1/2}$ , and  $\lambda$ ) have minimum values at low energies and then they increase as the photon energy increases, reaching their maximum values at the high energy level [49]. **Figure 7** describes the attenuation properties of the investigated flavonoid samples in terms of effective atomic number ( $Z_{eff}$ ) as a function of energy up to 15 MeV. Unlike the transmission factors, the highest  $Z_{eff}$  values indicate that the highest attenuation occurred in the investigated flavonoid samples [50–52]. Therefore, the highest  $Z_{eff}$  and then the highest attenuation occurred at the high energy level (15 keV) with values of 4.99, 5.83, 5.71, 6.13, 11.75, 6.38, 6.34, 6.45, and



6.48 for geraniol, betaine, thymoquinone, L-carnosine, N-acetylcysteine, apigenin, catechin, epigallocatechin, and saponarin, respectively. In radiation studies, the photon attenuation can be fully understood by determining two basic terms: attenuation factors (e.g., LAC, MAC, and TVL) and the buildup factors. In the previous section, we discuss in detail all the concepts related to the attenuation factors of the investigated flavonoid samples. Now, we shall throw light on the buildup factors of the investigated flavonoid samples. The buildup factors, namely, exposure buildup factor (EBF) and energy absorption buildup factor (EABF), were evaluated in the present research *via* the G-P fitting method based on Phy-X software. The fitting parameters and the required data for the calculations of EBF and EABF are summarized in **Supplementary Table S1**, **Supplementary Table S2**, **Supplementary Table S3**, **Supplementary Table S4**, **Supplementary Table S5**, **Supplementary Table S6**, **Supplementary Table S7**, **Supplementary Table S8**, and **Supplementary Table S9** for the investigated samples of geraniol, betaine, thymoquinone, L-carnosine, N-acetylcysteine, apigenin, catechin, epigallocatechin, and saponarin, respectively.

**Figure 8** and **Figure 9** depict the variation of EBF and EABF against photon energy for all studied flavonoid samples. Obviously, both EBF and EABF have a similar behavior (according to the dominant processes) against photon energy for various energy levels. Such that the highest buildup factors were observed in the middle energy levels, where the Compton scattering is the dominant process, while the lowest buildup

factors can be seen in the low and high energy levels where the photon absorption mechanism is a dominating process [53–56]. **Figure 10** and **Figure 11** demonstrate the variation of EBF and EABF against all studied flavonoid samples for photon energy of 0.4 MeV at various penetration depths (10, 20, 30, and 40 mfp). These figures show the extraordinary behavior of the buildup factors for the present flavonoid sample of N-acetylcysteine due to the existence of S element in the chemical composition of this sample. Such interesting observation supports the fundamental concepts of gamma interactions with matter. **Figure 12** shows a comparison between EBF and EABF and their variations with the effective atomic number and energy of 1 MeV and depth of 5 mfp. Clearly, EBF values are bigger than EABF values for all the effective atomic number less than 4.5 for all the investigated samples. However, there is a swift decrease for the effective atomic number higher than 4.5, for example, the present flavonoid sample of N-acetylcysteine. Finally, we shall briefly discuss the neutron attenuation features of the investigated flavonoid samples in terms of removal cross-section for fast neutron. **Figure 13** describes the neutron attenuation properties of the investigated flavonoid samples in terms of the removal cross section for fast neutron. One can see that the fast neutrons interact with the present sample with the cross-section values of 0.099, 0.099, 0.094, 0.111, 0.103, 0.105, 0.117, 0.122, and 0.133  $\text{cm}^{-1}$  for geraniol, betaine, thymoquinone, L-carnosine, N-acetylcysteine, apigenin, catechin, epigallocatechin, and saponarin, respectively. Therefore, the saponarin sample possesses the highest neutron cross-section among all the present samples.

## Molecular Properties

Molecular properties, including polar surface area, SASA, and heat of formation, were determined and compared with each other for all nine flavonoid compounds used in this study, as depicted in **Figure 14**. The molecular polar surface area is defined as the sum of the molecular surface overall polar atoms, including nitrogen and oxygen atoms with their attached hydrogen atoms. Evaluation of polar surface area of flavonoids clearly indicated that saponarin flavonoid has the largest polar surface area as compared to any other flavonoid used in this study with values of 20.23, 34.14, 40.12, 86.99, 105.19, 110.38, 121.1, 130.61, and 256.28 Å<sup>2</sup> for geraniol, thymoquinone, betaine, apigenin, N-acetylcysteine, catechin, L-carnosine, epigallocatechin, and saponarin, respectively, as shown in **Figure 14A**. This greater polar surface area of saponarin can be attributed to the presence of a higher number of oxygen atoms present in the chemical structure of saponarin compared to other flavonoids. At the same time, geraniol exhibited the least polar surface owing to the presence of only one polar atom in its chemical composition. Similarly, SASA of saponarin was also the largest with a more rigid structure due to the presence of a relatively higher number of aromatic rings than other flavonoids, as displayed in **Figure 14B**. The heat of formation for flavonoids was also compared, indicating that saponarin was the most stable one with a more negative heat of formation value of  $-565.71$  kcal/mol (**Figure 14C**). All these above-mentioned molecular properties clearly indicate that saponarin has the largest polar surface area and SASA, with more stability than other flavonoids.

## CONCLUSION

This study aimed to investigate a potential behavioral relation between chemical and physical properties of different types of flavonoids in terms of extending the information for the scientific community. Accordingly, geraniol, thymoquinone, betaine, apigenin, N-acetylcysteine, catechin, L-carnosine, epigallocatechin, and saponarin were extensively analyzed in terms of chemical and physical attitudes. The results showed that elemental compositions of the flavonoids have a direct impact on chemical and physical behaviors. Moreover, a synergistic effect was also reported between chemical and physical behaviors. Among the investigated flavonoids, saponarin was reported with the largest polar surface area and SASA, with more stability than other flavonoids. In addition, saponarin has the highest gamma-ray attenuation properties in large-scale photon energy. It can be concluded that the elemental structure of saponarin can provide a synergistic link between the chemical and physical properties. Considering the importance of such materials for the pharmaceutical and food industry, it can be suggested that the results obtained from this study can be useful

## REFERENCES

- Riley PA. Free Radicals in Biology: Oxidative Stress and the Effects of Ionizing Radiation. *Int J Radiat Biol* (1994) 65:27–33. doi:10.1080/09553009414550041

for the research and development activities of the industries in advanced applications. Therefore, the attributable properties of saponarin such as chemical composition, number of certain elements in its structure, and material density should always be considered.

## DATA AVAILABILITY STATEMENT

The original contributions presented in the study are included in the article/**Supplementary Material**, further inquiries can be directed to the corresponding authors.

## AUTHOR CONTRIBUTIONS

HT, MK, and SI were responsible for conceptualization. EK and HT developed the methodology. HT, HZ, EK, and AE contributed software. SI, MA, and AE undertook validation. HZ, MA, and BI performed formal analysis. WE and HT assisted with the investigation. MA and BI were responsible for resources. HZ, SI, and AE contributed to data curation. EK, MA-B, HT, and MA were responsible for writing—original draft preparation. HZ, SI, and AE undertook writing—review and editing. MK and MA-B performed visualization. HT and MK were responsible for supervision. MA-B, HT, and SI contributed to project administration. AE undertook funding acquisition. All authors have read and agreed to the published version of the manuscript.

## FUNDING

The authors express their sincere gratitude to Princess Nourah bint Abdulrahman University Researchers Supporting Project Number (PNURSP2022R149) and Princess Nourah bint Abdulrahman University, Riyadh, Saudi Arabia.

## ACKNOWLEDGMENTS

The APC was covered by “Dunarea de Jos” University of Galati, Romania. The researcher (HZ) is funded by a scholarship under the Joint (Executive Program between Egypt and Russia).

## SUPPLEMENTARY MATERIAL

The Supplementary Material for this article can be found online at: <https://www.frontiersin.org/articles/10.3389/fphy.2022.838725/full#supplementary-material>

- Cadenas E. Biochemistry of Oxygen Toxicity. *Annu Rev Biochem* (1989) 58: 79–110. doi:10.1146/annurev.bi.58.070189.000455
- Inoue M, Sato EF, Nishikawa M, Park A-M, Kira Y, Imada I, et al. Mitochondrial Generation of Reactive Oxygen Species and its Role in Aerobic Life. *Curr Med Chem* (2003) 10:2495–505. doi:10.2174/0929867033456477

4. Rahman K. Studies on Free Radicals, Antioxidants, and Co-factors. *Clin Interv Aging* (2007) 2:219–36. doi:10.1016/j.ceramint.2019.11.062
5. Mates JM, Pérez-Gómez C, De Castro IN. Antioxidant Enzymes and Human Diseases. *Clin Biochem* (1999) 32:595–603. doi:10.1016/S0009-9120(99)00075-2
6. McCall MR, Frei B. Can Antioxidant Vitamins Materially Reduce Oxidative Damage in Humans? *Free Radic Biol Med* (1999) 26:1034–53. doi:10.1016/S0891-5849(98)00302-5
7. Sies H, Stahl W, Sevanian A. Nutritional, Dietary and Postprandial Oxidative Stress. *J Nutr* (2005) 135:969–72. doi:10.1093/jn/135.5.969
8. Santos-Buelga C, Scalbert A. Proanthocyanidins and Tannin-like Compounds - Nature, Occurrence, Dietary Intake and Effects on Nutrition and Health. *J Sci Food Agric* (2000) 80:1094–117. doi:10.1002/(sici)1097-0010(20000515)80:7<1094::aid-jsfa569>3.0.co;2-1
9. Schroeter H, Boyd C, Spencer J, Williams R, Cadenas E, Riceevans C. MAPK Signaling in Neurodegeneration: Influences of Flavonoids and of Nitric Oxide. *Neurobiol Aging* (2002) 23:861–80. doi:10.1016/S0197-4580(02)00075-1
10. Rice-Evans C. Flavonoid Antioxidants. *Cmc* (2001) 8:797–807. doi:10.2174/0929867013373011
11. Peng XC, Huang JR, Wang SW, Liu L, Liu ZZ, Sethi G, et al. Traditional Chinese Medicine in Neuroprotection after Brain Insults with Special Reference to Radioprotection. *Evidence-Based Complement Altern Med* (2018) 2018:1–14. doi:10.1155/2018/2767208
12. Betlazar C, Middleton RJ, Banati RB, Liu G-J. The Impact of High and Low Dose Ionising Radiation on the central Nervous System. *Redox Biol* (2016) 9:144–56. doi:10.1016/j.redox.2016.08.002
13. Balcer-Kubiczek EK. The Role of the Apoptotic Machinery in Ionizing Radiation-Induced Carcinogenesis. *Crit Rev Oncog* (2016) 21:169–84. doi:10.1615/CritRevOncog.2016016984
14. Kivrak E, Yurt K, Kaplan A, Alkan I, Altun G. Effects of Electromagnetic fields Exposure on the Antioxidant Defense System. *J Microsc Ultrastruct* (2017) 5:167. doi:10.1016/j.jmau.2017.07.003
15. Boice JD. Studies of Atomic Bomb Survivors. Understanding Radiation Effects. *J Am Med Assoc* (1990) 264:622–3. doi:10.1001/jama.264.5.622
16. Wang SW, Ren BX, Qian F, Luo XZ, Tang X, Peng XC, et al. Radioprotective Effect of Epimedium on Neurogenesis and Cognition after Acute Radiation Exposure. *Neurosci Res* (2019) 145:46–53. doi:10.1016/j.neures.2018.08.011
17. Alterio D, Marvaso G, Ferrari A, Volpe S, Orecchia R, Jereczek-Fossa BA. Modern Radiotherapy for Head and Neck Cancer. *Semin Oncol* (2019) 46:233–45. doi:10.1053/j.seminoncol.2019.07.002
18. Ho JC, Phan J. Reirradiation of Head and Neck Cancer Using Modern Highly Conformal Techniques. *Head & Neck* (2018) 40:2078–93. doi:10.1002/hed.25180
19. Burns TC, Awad AJ, Li MD, Grant GA. Radiation-induced Brain Injury: Low-Focusing Fruit for Neuroregeneration. *Foc* (2016) 40:E3. doi:10.3171/2016.2.FOCUS1611
20. Fischer N, Seo E-J, Efferth T. Prevention from Radiation Damage by Natural Products. *Phytomedicine* (2018) 47:192–200. doi:10.1016/j.phymed.2017.11.005
21. Wang Q, Xie C, Xi S, Qian F, Peng X, Huang J, et al. Radioprotective Effect of Flavonoids on Ionizing Radiation-Induced Brain Damage. *Molecules* (2020) 25:5719. doi:10.3390/molecules25235719
22. Medeiros KAAL, dos Santos JR, Melo TCd. S, de Souza MF, Santos Ld. G, de Gois AM, et al. Depressant Effect of Geraniol on the central Nervous System of Rats: Behavior and ECoG Power Spectra. *Biomed J* (2018) 41:298–305. doi:10.1016/j.bj.2018.08.008
23. Barak AJ, Beckenhauer HC, Tuma DJ. Use of S-Adenosylmethionine as an index of Methionine Recycling in Rat Liver Slices. *Anal Biochem* (1982) 127:372–5. doi:10.1016/0003-2697(82)90189-0
24. Ganesan B, Anandan R, Lakshmanan PT. Studies on the Protective Effects of Betaine against Oxidative Damage during Experimentally Induced Restraint Stress in Wistar Albino Rats. *Cell Stress and Chaperones* (2011) 16:641–52. doi:10.1007/s12192-011-0276-4
25. Abdelmeguid NE, Fakhoury R, Kamal SM, Al Wafai RJ. Effects of Nigella Sativa and Thymoquinone on Biochemical and Subcellular Changes in Pancreatic  $\beta$ -cells of Streptozotocin-Induced Diabetic Rats. *J Diabetes* (2010) 2:256–66. doi:10.1111/j.1753-0407.2010.00091.x
26. Saeed Al-Zahrani S, Mohany M, Kandeal S, Badr G. Thymoquinone and Vitamin E Supplementation Improve the Reproductive Characteristics of Heat Stressed Male Mice. *J Med Plants Res* (2012) 6:493–9. doi:10.5897/JMPR11.1252
27. Abdelkader H, Longman M, Alany RG, Pierscionek B. On the Anticataractogenic Effects of L-Carnosine: Is it Best Described as an Antioxidant, Metal-Chelating Agent or Glycation Inhibitor? *Oxidative Med Cell Longevity* (2016) 2016:1–11. doi:10.1155/2016/3240261
28. Kim Y, Kim Y. L-histidine and L-Carnosine Exert Anti-brain Aging Effects in D-Galactose-Induced Aged Neuronal Cells. *Nutr Res Pract* (2020) 14:188–202. doi:10.4162/nrp.2020.14.3.188
29. Żukowski P, Maciejczyk M, Matczuk J, Kurek K, Waszkiel D, Żendzian-Piotrowska M, et al. Effect of N-Acetylcysteine on Antioxidant Defense, Oxidative Modification, and Salivary Gland Function in a Rat Model of Insulin Resistance. *Oxidative Med Cell Longevity* (2018) 2018:1–11. doi:10.1155/2018/6581970
30. Zhang Q, Ju Y, Ma Y, Wang T. N-acetylcysteine Improves Oxidative Stress and Inflammatory Response in Patients with Community Acquired Pneumonia. *Med (United States)* (2018) 97:e13087. doi:10.1097/MD.00000000000013087
31. Sánchez-Marzo N, Pérez-Sánchez A, Ruiz-Torres V, Martínez-Tébar A, Castillo J, Herranz-López M, et al. Antioxidant and Photoprotective Activity of Apigenin and its Potassium Salt Derivative in Human Keratinocytes and Absorption in Caco-2 Cell Monolayers. *Ijms* (2019) 20:2148. doi:10.3390/ijms20092148
32. Zhang J, Zhao X, Zhu H, Wang J, Ma J, Gu M. Apigenin Protects against Renal Tubular Epithelial Cell Injury and Oxidative Stress by High Glucose via Regulation of NF-E2-Related Factor 2 (Nrf2) Pathway. *Med Sci Monit* (2019) 25:5280–8. doi:10.12659/MSM.915038
33. Simeonova R, Vitcheva V, Kondeva-Burdina M, Krasteva I, Manov V, Mitcheva M. Hepatoprotective and Antioxidant Effects of Saponarin, Isolated from *Gypsophila trichotoma* Wend. On Paracetamol-Induced Liver Damage in Rats. *Biomed Res Int* (2013) 2013:1–10. doi:10.1155/2013/757126
34. Mezera V, Kučera O, Moravcová A, Peterová E, Červinková Z. Epigallocatechin Gallate Does Not Accelerate the Early Phase of Liver Regeneration after Partial Hepatectomy in Rats. *Dig Dis Sci* (2014) 59:976–85. doi:10.1007/s10620-013-2966-5
35. Botten D, Fugallo G, Fraternali F, Molteni C. Structural Properties of Green Tea Catechins. *J Phys Chem B* (2015) 119:12860–7. doi:10.1021/acs.jpcc.5b08737
36. RSICC. RSICC Computer Code Collection, MCNPX User's Manual Version 2.4.0. MonteCarlo N-Particle Transport Code System for Multiple and High Energy Applications (2002). Available at: [https://www.google.com/search?q=RSICC+Computer+Code+Collection%2C+MCNPX+User%27s+Manual+Version+2.4.0.+MonteCarlo+N-Particle+Transport+Code+System+for+Multiple+and+High+Energy+Applications%2C\(2002\).&sq=RSICC+Computer+Code+Collection%2C+MCNPX+User%27s+Manu](https://www.google.com/search?q=RSICC+Computer+Code+Collection%2C+MCNPX+User%27s+Manual+Version+2.4.0.+MonteCarlo+N-Particle+Transport+Code+System+for+Multiple+and+High+Energy+Applications%2C(2002).&sq=RSICC+Computer+Code+Collection%2C+MCNPX+User%27s+Manu) (Accessed December 31, 2020).
37. Voityuk AA, Rösch N. AM1/d Parameters for Molybdenum. *J Phys Chem A* (2000) 104:4089–94. doi:10.1021/jp994394w
38. Kavaz E, Ahmadishadbad N, Özdemir Y. Photon Buildup Factors of Some Chemotherapy Drugs. *Biomed Pharmacother* (2015) 69:34–41. doi:10.1016/j.biopha.2014.10.031
39. Ekinci N, Kavaz E, Özdemir Y. A Study of the Energy Absorption and Exposure Buildup Factors of Some Anti-inflammatory Drugs. *Appl Radiat Isot* (2014) 90:265–73. doi:10.1016/j.apradiso.2014.05.003
40. Tekin HO, Karahan M, Erguzel TT, Manici T, Konuk M. Radiation Shielding Parameters of Some Antioxidants Using Monte Carlo Method. *J Biol Phys* (2018) 44:579–90. doi:10.1007/s10867-018-9507-6
41. Tekin HO, Sayyed MI, Kilicoglu O, Karahan M, Erguzel TT, Kara U, et al. Calculation of Gamma-ray Attenuation Properties of Some Antioxidants Using Monte Carlo Simulation Method. *Biomed Phys Eng Express* (2018) 4:057001. doi:10.1088/2057-1976/aad297
42. Zakaly HMH, Saudi HA, Issa SAM, Rashad M, Elazaka AI, Tekin HO, et al. Alteration of Optical, Structural, Mechanical Durability and Nuclear Radiation Attenuation Properties of Barium Borosilicate Glasses through BaO Reinforcement: Experimental and Numerical Analyses. *Ceramics Int* (2021) 47:5587–96. doi:10.1016/j.ceramint.2020.10.143

43. Akkurt I, Boodaghi Malidarre R. Gamma Photon-Neutron Attenuation Parameters of marble concrete by MCNPX Code. *Radiat Effects Defects Sol* (2021) 176:906–18. doi:10.1080/10420150.2021.1975708
44. Akkurt I, Tekin HO. Radiological Parameters of Bismuth Oxide Glasses Using the Phy-X/PSD Software. *Emerging Mater Res* (2020) 9:1020–7. doi:10.1680/jemmr.20.00209
45. Rammah YS, Kumar A, Mahmoud KA-A, El-Mallawany R, El-Agawany FI, Susoy G, et al. SnO-reinforced Silicate Glasses and Utilization in Gamma-Radiation-Shielding Applications. *Emerging Mater Res* (2020) 9:1000–8. doi:10.1680/jemmr.20.00150
46. Tekin HO, Issa SAM, Mahmoud KA-A, El-Agawany FI, Rammah YS, Susoy G, et al. Nuclear Radiation Shielding Competences of Barium-Reinforced Borosilicate Glasses. *Emerging Mater Res* (2020) 9:1131–44. doi:10.1680/jemmr.20.00185
47. Çelen YY. Gamma-ray-shielding Parameters of Some Phantom Fabrication Materials for Medical Dosimetry. *Emerging Mater Res* (2021) 10:307–13. doi:10.1680/jemmr.21.00043
48. Zakaly HMH, Rashad M, Tekin HO, Saudi HA, Issa SAM, Henaish AMA. Synthesis, Optical, Structural and Physical Properties of Newly Developed Dolomite Reinforced Borate Glasses for Nuclear Radiation Shielding Utilizations: An Experimental and Simulation Study. *Opt Mater* (2021) 114:110942. doi:10.1016/j.optmat.2021.110942
49. Çelen YY, Evcin A. Synthesis and Characterizations of Magnetite-Borogypsum for Radiation Shielding. *Emerging Mater Res* (2020) 9:770–5. doi:10.1680/jemmr.20.00098
50. Lakshminarayana G, Kumar A, Tekin HO, Issa SAM, Al-Buriahi MS, Dong MG, et al. Illustration of Distinct Nuclear Radiation Transmission Factors Combined with Physical and Elastic Characteristics of Barium Boro-Bismuthate Glasses. *Results Phys* (2021) 31:105067. doi:10.1016/j.rinp.2021.105067
51. Ilik E, Kavaz E, Kilic G, Issa SAM, AlMisned G, Tekin HO. Synthesis and Characterization of Vanadium(V) Oxide Reinforced Calcium-Borate Glasses: Experimental Assessments on Al<sub>2</sub>O<sub>3</sub>/BaO<sub>2</sub>/ZnO Contributions. *J Non-Crystalline Sol* (2022) 580:121397. doi:10.1016/j.jnoncrysol.2022.121397
52. Lakshminarayana G, Kumar A, Tekin HO, Issa SAM, Al-Buriahi MS, Dong MG, et al. Probing of Nuclear Radiation Attenuation and Mechanical Features for Lithium Bismuth Borate Glasses with Improving Bi<sub>2</sub>O<sub>3</sub> Content for B<sub>2</sub>O<sub>3</sub> + Li<sub>2</sub>O Amounts. *Results Phys* (2021) 25:104246. doi:10.1016/j.rinp.2021.104246
53. AlMisned G, Elshami W, Issa S, Susoy G, Zakaly H, Algethami M, et al. Enhancement of Gamma-ray Shielding Properties in Cobalt-Doped Heavy Metal Borate Glasses: The Role of Lanthanum Oxide Reinforcement. *Materials* (2021) 14:7703. doi:10.3390/MA14247703
54. Lakshminarayana G, Kumar A, Tekin HO, Issa SAM, Al-Buriahi MS, Lee D-E, et al. Binary B<sub>2</sub>O<sub>3</sub>-Bi<sub>2</sub>O<sub>3</sub> Glasses: Scrutinization of Directly and Indirectly Ionizing Radiations Shielding Abilities. *J Mater Res Tech* (2020) 9:14549–67. doi:10.1016/j.jmrt.2020.10.019
55. Mostafa AMA, Issa SAM, Zakaly HMH, Zaid MHM, Tekin HO, Matori KA, et al. The Influence of Heavy Elements on the Ionizing Radiation Shielding Efficiency and Elastic Properties of Some Tellurite Glasses: Theoretical Investigation. *Results Phys* (2020) 19:103496. doi:10.1016/j.rinp.2020.103496
56. Zakaly HM, Ashry A, El-Taher A, Abbady AGE, Allam EA, El-Sharkawy RM, et al. Role of Novel Ternary Nanocomposites Polypropylene in Nuclear Radiation Attenuation Properties: In-Depth Simulation Study. *Radiat Phys Chem* (2021) 188:109667. doi:10.1016/j.radphyschem.2021.109667

**Conflict of Interest:** The authors declare that the research was conducted in the absence of any commercial or financial relationships that could be construed as a potential conflict of interest.

**Publisher's Note:** All claims expressed in this article are solely those of the authors and do not necessarily represent those of their affiliated organizations, or those of the publisher, the editors, and the reviewers. Any product that may be evaluated in this article, or claim that may be made by its manufacturer, is not guaranteed or endorsed by the publisher.

Copyright © 2022 Tekin, AlMisned, Issa, Kasikci, Arooj, Ene, Al-Buriahi, Konuk and Zakaly. This is an open-access article distributed under the terms of the Creative Commons Attribution License (CC BY). The use, distribution or reproduction in other forums is permitted, provided the original author(s) and the copyright owner(s) are credited and that the original publication in this journal is cited, in accordance with accepted academic practice. No use, distribution or reproduction is permitted which does not comply with these terms.